A Novel Method for Modeling Dynamic Air-Gap Eccentricity in Synchronous Machines Based on Modified Winding Function Theory

Nabil A. Al-Nuaim
Student Member, IEEE

Hamid A. Toliyat
Senior Member, IEEE

Department of Electrical Engineering
Texas A&M University
College Station, TX 77843-3128
Fax : (409) 845-6259

Abstract- This paper presents the modeling of synchronous machines under eccentric rotors. The winding function theory accounting for all space harmonics and presented by earlier researchers has been modified to adopt non-symmetric air-gap for the calculation of machine winding inductances. The effect of dynamic air-gap eccentricity on the inductances of a salient-pole synchronous machine using the modified winding function approach (MWFA) has been discussed. Coupled magnetic circuits approach has been used for simulating the machine behavior under healthy and eccentric rotor conditions. The simulation results are in close agreement with the experimental results.

Keywords: Winding function theory, dynamic eccentricity, synchronous machines, motor current signature analysis.

I. INRTODUCTION

Rotating electrical machines play a very important role in the world's industrial life. In petrochemical and power utilities, the failure of critical rotating machines, such as electric motors and generators cost millions of dollars. This is due to the loss of production, high emergency maintenance costs and lost revenues. Industry's response towards this problem of unexpected interruptions of work is by using "catch it before it fails" approach. So, the industry started investing heavily on preventive maintenance programs, that is, detecting machine problems before they can result in catastrophic failures [1].

The oldest technique for preventive maintenance was tearing the electrical machine down and then looking at it closely. However, taking the motor out of service is costly and time consuming. This is why today's modern industry management is more interested than ever before in adopting new condition monitoring techniques, on-line or off-line, to assess and evaluate the rotating electrical machine's performance condition.

Electric machines can operate under asymmetrical conditions due to mechanical and/or electrical irregularities. These asymmetrical conditions can be summarized in the following:

PE-718-EC-0-05-1997 A paper recommended and approved by the IEEE Electric Machinery Committee of the IEEE Power Engineering Society for publication in the IEEE Transactions on Energy Conversion. Manuscript submitted November 26, 1996; made available for printing May 23, 1997.

- Broken rotor bars or cracked rotor end-ring.
- Inter-turn fault resulting in the shorting or opening of one or more circuits of a stator phase winding.
- Rotor eccentricities. A rub between the rotor and the stator core can result in serious damage to the stator and rotor windings and cores.
- Short in rotor field windings in the case of synchronous machines causing overheating which may also result in bending of the rotor.

Recent efforts in fault diagnosis include electrical, mechanical, chemical, and magnetic techniques [2]. These techniques are the basis for developing on-line and/or off-line rotating electrical machine condition monitoring systems. Electrical and magnetic techniques include magnetic flux measurement, stator current analysis, rotor current analysis, partial discharges for evaluating stator insulation strength for high voltage motors, shaft induced voltages, etc. Mechanical techniques include the machine bearing vibration monitoring systems, speed fluctuation analysis of induction machines and bearing temperature measurement. One of the chemical techniques used is the carbon monoxide gas analysis due to degradation of electrical insulation for closed circuit air cooled motors with water cooled heat exchangers. Another chemical technique is the analysis of bearing oil.

It is beyond the objective of this paper to cover in detail different monitoring techniques for detecting various faults on large machines. However, one of the electrical techniques, namely motor current signature analysis, will be used to study the effect of rotor dynamic eccentricity on synchronous motors. In the next section, some of the previous efforts accomplished to detect rotor eccentricity on large ac machines will be briefly reviewed.

Several authors have examined the effect of rotor eccentricity on machine parameters and performance. Different ways to model and to monitor the machines with air-gap eccentricity have been developed. There is a large number of published articles on this subject for induction machines and relatively fewer for synchronous machines. In this paper, several related ones will be reviewed.

Cameron et al. [3] have presented the detection of air-gap eccentricity for large induction motors by selecting the line current and motor frame vibration as the monitored parameters. For the line current harmonics analysis, the magnetomotive force (MMF), and the resultant air-gap permeance including rotor and stator slotting, saturation and eccentricity were presented. Then, the flux density distribution in the air gap was computed by the product of permeance and the MMF. The harmonic content in the flux density waveform was investigated and concluded that since the harmonic fluxes move relative to the stator, then, they should induce corresponding current harmonics in the stationary stator windings.

Dorrell et al. [4] presented a similar paper on the analysis of air-gap flux, current and vibration signals as a function of both static and dynamic air-gap eccentricity in 3-phase induction motors. They used the same approach, the air-gap permeance approach, as in [3] for calculating the flux density and unbalanced magnetic forces caused by eccentricity; except that they suggested that the dynamic and static eccentricity should both be considered simultaneously and a new theoretical analysis was presented. Also, it was suggested that in addition to monitoring the line current signature, the vibration analysis should be put forward to identify which particular form of eccentricity is dominant.

Vas [5] even went further and presented a formula for computing the frequency components in the stator currents of an induction machine which is due to air-gap eccentricity. The frequency components are found to be a function of the fundamental stator frequency, number of rotor slots, slip, type of eccentricity and stator MMF time harmonics.

Verma and Natarajan [6] have studied the changes in the air-gap field as a function of static eccentricity using search coils in the stator core. However, the installation of air-gap search coils is neither practical nor economical for monitoring the condition of the motors that are already in service such as the ones existing in off-shore installations.

Toliyat et al. [7] have also proposed the detection of air-gap eccentricity in induction machines by measuring the harmonic content in the machine line currents. However, they proposed a new way for modeling the machine under eccentricity. The winding function approach accounting for all the space harmonics in the machine was used to calculate all the mutual and magnetizing inductances for the induction machine with eccentric rotors.

There are fewer publications on the detection of rotor eccentricity using electrical techniques for synchronous machines. Htsui, and Stein [8] have proposed using the shaft voltage signals generated by the shaft flux linkages to detect eccentricities and shorted rotor field in synchronous machines. The magnitude and the thickness of the shaft signal loci reflect static and dynamic eccentricities.

The interest in the condition monitoring, on-line and/or off-line, of ac machines has increased tremendously in the last few years because of economic pressures, smaller profit margins and high costs of replacement and spare parts. Therefore, in order to achieve this goal, it is very important to be able to develop simple models for the machines under fault conditions and then analyze the effect of faults on the machines' behavior. This study is an attempt toward this goal.

In this paper, a new linear model, i.e. saturation not included, for synchronous machines by using the geometry and the physical layout of all windings will be developed. This model can be used to simulate the machine under fault conditions such as air-gap eccentricity. The developed model will be used to investigate the effect of dynamic air-gap eccentricity on the stator and rotor magnetizing and mutual inductances of a salient-pole synchronous motor.

Finally, the stator current signature patterns of the linear model will be examined to find specific harmonic components that are related to dynamic air-gap eccentricity.

The winding function approach accounting for all space harmonics in the machine will be used to compute all of the relevant inductances of the stator phases and the rotor field windings of the salient-pole synchronous machine. The inductances will be computed for both cases, when the rotor does and does not experience air-gap eccentricity. In the case of eccentric rotors, the air-gap is not uniform. Therefore, a new formulation for computing the inductances has to be developed.

II. THE MODIFIED WINDING FUNCTION APPROACH (MWFA)

All conventional machines rely upon magnetic fields for the purpose of energy conversion. Windings are arranged on a stationary member (stator) and on the rotating member (rotor) so as to set up a field distribution of magnetic flux density in the space which separates the stator from the rotor (air-gap). Working directly with the electromagnetic fields as an approach to study electrical machines leads to a better understanding of flux, current density, and force distributions in the machine, moreover where hot spots might appear. However, the analysis of machines as a magnetic field problem needs extensive digital computer horsepower. The geometry of electric machines normally leads to complicated boundary conditions even for simplified models. For this reason, it is more convenient and the problem will be much more simplified if coupled magnetic circuits approach is used.

An elementary two-pole, salient-pole synchronous machine shown in Figs. 1 with an eccentric rotor will be used for developing the modified winding function approach (MWFA). A single conductor is threaded back and forth in the gap forming the total number of turns for the winding which need not be associated with either the stator or rotor at this point. The stator shape is assumed to be cylindrical . Also, the permeability of the stator and rotor iron cores is assumed to be infinite when compared to the permeability of the air-gap.

The stator reference position, the angle φ, of the closed path *abcda* of Fig. 1 is taken at an arbitrary point along the gap. Points *a* and *d* are located on the stator corresponding to angles 0 and φ respectively and points *b* and *c* are located on the rotor. In the case of salient-pole synchronous machines, the flux lines will take irregular paths in the air-gap but intersect with the stator and rotor at right angles. Therefore, paths ab and cd are defined to lie along the lines of flux even though these flux lines cannot be uniquely defined without using flux plots. However, using Gauss's law for magnetic fields, points b and c are uniquely defined since two flux lines can never originate from the same point if points a and d are fixed on the stator.

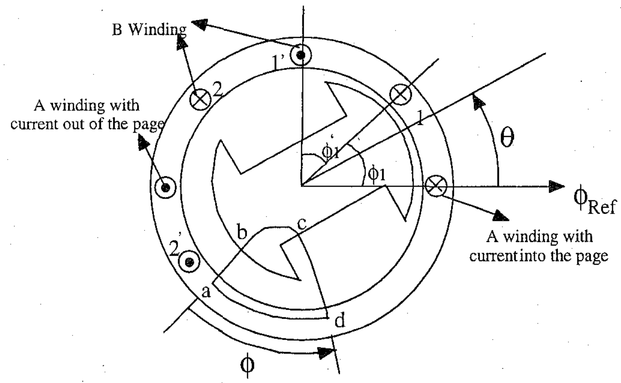

Fig. 1. Elementary salient-pole machine with symmetric placement of windings in the gap and eccentric rotor.

Consider the path $abcda$ of Fig. 1 for an arbitrary $0<\varphi<2\pi$, by Ampere's law

$$\oint_{abcda} H.dl = \int_S J.dS \tag{1}$$

where S is the surface enclosed by the path $abcda$. Since all the windings enclosed by the closed path carry the same current i, (1) reduces to the following:

$$\oint_{abcda} H.dl = n(\varphi,\theta).\, i \tag{2}$$

where H is the magnetic field intensity and dl is defined to be along the flux lines originating or terminating at two points of the closed path $abcda$. The function $n(\varphi,\theta)$ is called the ***turns function*** and represents the number of turns of the winding enclosed by the path $abcda$. In general, for a rotating coil it is assumed to be a function of φ and the rotor position angle θ. For a stationary coil it is only a function of φ. Turns carrying currents i into the page are considered positive while the turns carrying currents i out of the page are considered negative. In terms of MMF drops in a magnetic circuit, (2) can be written

$$F_{ab} + F_{bc} + F_{cd} + F_{da} = n(\varphi,\theta).\, i \tag{3}$$

Since the iron is considered to be infinitely permeable, the MMF drops F_{bc} and F_{da} are negligible and (3) reduces to

$$F_{ab}(0,\theta) + F_{cd}(\varphi,\theta) = n(\varphi,\theta).\, i \tag{4}$$

Gauss's law for magnetic field can be used to find an expression for the MMF drop at $\varphi = 0$, $F_{ab}(0,\theta)$, which is given by

$$\oint_S B.dS = 0 \tag{5}$$

where B represents magnetic flux density and the surface integral is carried out over the boundary surface of an arbitrary volume. Taking the surface S to be a cylindrical volume located just inside the stator inner surface, (5) can be written as

$$\int_0^{2\pi}\int_0^{L} \mu_0 H(\varphi,\theta).\, r(dl)(d\varphi) = 0 \tag{6}$$

where L is the axial stack length of the machine, r is the stator inner radius, μ_0 is the free space permeability and θ is the angular position of the rotor with respect to stator. Since B does not vary with respect to the axial length, and MMF is the product of flux radial length and the magnetic field intensity, then

$$\int_0^{2\pi} \frac{F(\varphi,\theta)}{g(\varphi,\theta)}\, d\varphi = 0 \tag{7}$$

Dividing equation (4) by the ***air-gap function*** $g(\varphi,\theta)$, and then integrating from 0 to 2π yields

$$\int_0^{2\pi} \frac{F_{ab}(0,\theta) + F_{cd}(\varphi,\theta)}{g(\varphi,\theta)}\, d\varphi = \int_0^{2\pi} \frac{n(\varphi,\theta)}{g(\varphi,\theta)}\, i\, d\varphi \tag{8}$$

Since the second term of the left hand side is zero as found from Gauss's law, (8) will reduce to the following

$$F_{ab}(0,\theta) = \frac{1}{2\pi < g^{-1}(\varphi,\theta) >} \int_0^{2\pi} n(\varphi,\theta)\, g^{-1}(\varphi,\theta)\, i\, d\varphi \tag{9}$$

where $< g^{-1} >$ is the average value of the inverse gap function. Substituting (9) in (4) and solving for $F_{cd}(\varphi)$ yields

$$F_{cd}(\varphi,\theta) = \left[n(\varphi,\theta) - \frac{1}{2\pi < g^{-1}(\varphi,\theta) >} \int_0^{2\pi} n(\varphi,\theta)\, g^{-1}(\varphi,\theta)\, d\varphi \right] . i \tag{10}$$

From the last equation, the ***modified winding function***, in general, can be defined as follows

$$M(\varphi,\theta) = n(\varphi,\theta) - < M(\theta) > \tag{11}$$

where

$$< M(\theta) > = \frac{1}{2\pi < g^{-1}(\varphi,\theta) >} \int_0^{2\pi} n(\varphi,\theta)\, g^{-1}(\varphi,\theta)\, d\varphi \tag{12}$$

If the rotor is not eccentric , i.e. the air-gap is symmetric, and the north and south poles of the salient-pole machine are identical, then the inverse air-gap function $g^{-1}(\varphi,\theta)$ has only even harmonics including a dc value. Also, for practical machines, the windings are distributed in such a way that the turns function $n(\varphi,\theta)$ has only odd harmonics. Therefore, in the cases where the air-gap has only even harmonics, i.e. non-eccentric rotor, (12) reduces to

$$< M(\theta) > = < n > \tag{13}$$

where $< n >$ is the dc value of the turns function of the winding.

III. INDUCTANCE CALCULATIONS

In the previous section, the relative permeability of the iron was assumed to be infinity, i.e. the MMF drop in the iron was neglected. The MMF distribution of machine windings in the air gap can simply be found by product of the modified winding function calculated from (11) and the current flowing in the winding.

As shown in Fig. 1, windings A and B are located in the air gap and could be associated with either the rotor or the stator. The mutual inductance of winding B due to current i_A flowing in winding A is to be calculated. Winding B is arranged arbitrarily in the air gap and for demonstration is assumed to have two coil sides, 1-1' and 2-2', with different turns distribution in the air gap. The reference angle φ cannot be selected freely and should be the same reference position that has been previously used to calculate the modified winding function $M_A(\varphi,\theta)$.

The MMF distribution in the air gap due to current i_A can be calculated as follows

$$F_A(\varphi,\theta) = M_A(\varphi,\theta)\,.i_A \tag{14}$$

It is known that the flux in a magnetic circuit is the product of the MMF (F) and the permeance (P) of the flux path. Thus,

$$\Phi = F\,.\,P \tag{15}$$

and the permeance is given by

$$P = \frac{\mu\, A}{l} \tag{16}$$

where μ is the permeability, A is the cross sectional area and l is the length of the magnetic path. The differential flux across the gap through a differential volume of length $g(\varphi,\theta)$ and cross-sectional area of $(r.L.d\varphi)$ from the rotor to the stator is

$$d\Phi = F_A(\varphi,\theta)\,\mu_o\, r\, L \frac{d\varphi}{g(\varphi,\theta)} \tag{17}$$

The flux linking the coil sides 1-1' of winding B can be calculated using the following integration

$$\Phi_{1-1'} = \mu_0\, r\, L \int_0^{2\pi} n_{B1}(\varphi,\theta)\, F_A(\varphi,\theta)\, g^{-1}(\varphi,\theta)\, d\varphi \tag{18}$$

where $n_{B1}(\varphi,\theta)$ is equal to the number of turns of coil sides 1-1' between the reference angles φ_1 and φ'_1 of Fig. 1 and zero otherwise. Coil side 1' is the return path for coil side 1. Continuing the process of calculating the flux linking the other coil sides of winding B and in general for any set of coil sides k-k' the flux linkage is

$$\Phi_{k-k'} = \mu_0\, r\, L \int_0^{2\pi} n_{Bk}(\varphi,\theta)\, F_A(\varphi,\theta)\, g^{-1}(\varphi,\theta)\, d\varphi \tag{19}$$

where $n_{Bk}(\varphi,\theta)$, $F_A(\varphi,\theta)$ and $g^{-1}(\varphi,\theta)$ must have the same position reference φ. The total flux linking winding B due to current in winding A can be defined as follows

$$\lambda_{BA} = \sum_{k=1}^{q_i} \Phi_{k-k'} = \mu_0\, r\, L \left[\sum_{k=1}^{q_i} \int_0^{2\pi} n_{Bk}(\varphi,\theta) F_A(\varphi,\theta)\, g^{-1}(\varphi,\theta)\, d\varphi \right] \tag{20}$$

or

$$\lambda_{BA} = \mu_0\, r\, L \int_0^{2\pi} \left[\sum_{k=1}^{q_i} n_{Bk}(\varphi,\theta) \right] F_A(\varphi,\theta)\, g^{-1}(\varphi,\theta)\, d\varphi \tag{21}$$

where

$$n_B(\varphi,\theta) = \left[\sum_{k=1}^{q_i} n_{Bk}(\varphi,\theta) \right] \tag{22}$$

is the turns function for the winding B assuming that the q_i coil sides are connected in series and q_i can be defined as follows for the salient-pole synchronous machines:

$$q_s = \frac{\text{stator slots number}}{\text{phase number}} \times \frac{\text{number of layers}}{2}$$

for the stator windings and

$$q_r = \text{number of poles}$$

for rotor field windings. The mutual inductance L_{BA} of winding B due to the current i_A in winding A would be

$$L_{BA} = \frac{\lambda_{BA}}{i_A} = \mu_0\, r\, L \int_0^{2\pi} n_B(\varphi,\theta)\, M_A(\varphi,\theta)\, g^{-1}(\varphi,\theta)\, d\varphi \tag{23}$$

Using the same process, the magnetizing inductance of winding A can be defined as

$$L_{AA} = \mu_0\, r\, L \int_0^{2\pi} n_A(\varphi,\theta)\, M_A(\varphi,\theta)\, g^{-1}(\varphi,\theta)\, d\varphi \tag{24}$$

IV. INDUCTANCE CALCULATIONS UNDER DYNAMIC ECCENTRICITY

In general, rotor eccentricity in motors takes two forms, namely static air-gap eccentricity and dynamic air-gap eccentricity. In the case of *static air-gap eccentricity*, the position of minimum radial air-gap length is fixed in space and the center of rotation and the center of rotor are the same. For example, static eccentricity can be caused by oval stator cores or by the incorrect positioning of the stator or rotor. However, in the case of *dynamic air-gap eccentricity*, the center of rotation and the center of the rotor are not the same and the minimum air-gap rotates with the rotor. So, dynamic eccentricity is both time and space dependent. Dynamic eccentricity can be caused by misalignment of bearings, mechanical resonance at critical speeds, a bent rotor shaft, wear of bearings and so on [3]. In this paper, the inductances of a salient, 3-phase, four-pole synchronous machine whose parameters are given in the Appendix including the effect of dynamic eccentricity will be calculated.

Fig.2 illustrates the stator phase a turns function. The ac component of the phases b and c turns functions are the same as phase a except that they are shifted by 60° and 120° mechanical degrees respectively.

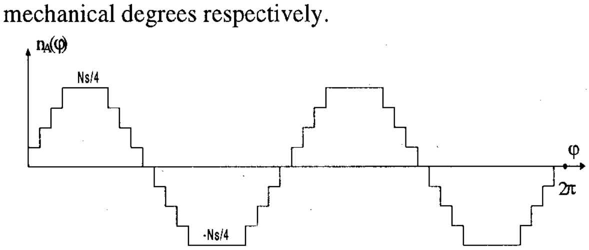

Fig. 2. Stator phase a turns function.

The rotor field turns function can be found similarly except that it is not stationary. The rotor position with respect to the previously selected reference angle φ is presented in Fig. 3 by the mechanical angle θ_m.

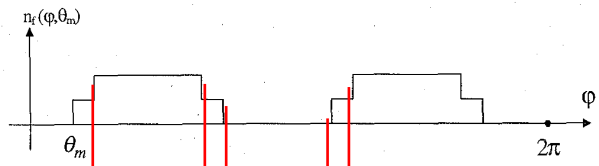

Fig. 3. Rotor field turns function.

The inverse gap functions of both rotor configurations when the rotor is and is not experiencing dynamic eccentricity are shown in Figs. 4 and 5. Similar to the rotor turns function, the inverse gap function is expressed by the rotor position angle θ_m since it is a function of rotor position too.

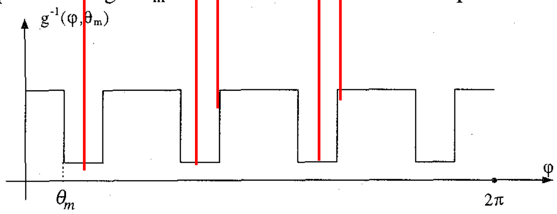

Fig. 4. Inverse gap function in case of symmetric rotor.

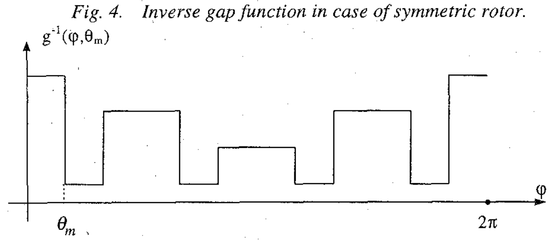

Fig. 5. Inverse gap function in case of non-symmetric rotor.

In this study, the inductances of the salient-pole synchronous machine with dynamic eccentricity will be calculated by expressing the turns functions, modified winding functions, and inverse gap function in their Fourier series representations. The Fourier series approach proves to be a vital tool since it makes the inductances of the machine under failure easier to analyze and interpret. The stator and rotor modified winding functions can be written in terms of their trigonometric cosine functions as follow:

$$M_A(\varphi,\theta_m) = -< M_A(\theta_m) > + < n_A > + \sum_{k=p\times odd}^{\infty} A_k \cos(k(\varphi+\delta)) \tag{25}$$

$$M_B(\varphi,\theta_m) = -< M_B(\theta_m) > + < n_B > + \sum_{k=p\times odd}^{\infty} A_k \cos\left(k(\varphi - \frac{2\pi}{3p} + \delta)\right) \tag{26}$$

$$M_C(\varphi,\theta_m) = -< M_C(\theta_m) > + < n_C > + \sum_{k=p\times odd}^{\infty} A_k \cos\left(k(\varphi + \frac{2\pi}{3p} + \delta)\right) \tag{27}$$

$$M_f(\varphi,\theta_m) = -< M_f > + < n_f > + \sum_{k=p\times odd}^{\infty} F_k \cos(k(\varphi - \theta_m + \gamma)) \tag{28}$$

where p is the number of pole pairs, δ and γ are phase shift angles found according to the selected stationary reference frame angle φ to be consistent for all geometrical functions. The inverse gap function can be expressed in the general form including dynamic eccentricity as follows:

$$g^{-1}(\varphi,\theta_m) = < g^{-1} > + \sum_{j=1}^{\infty} G_j \cos(j(\varphi - \theta_m + \lambda)) \tag{29}$$

where ($j = p$ x *even harmonics)* for non-eccentric rotor and (j = *all harmonics)* for dynamic eccentricity where λ is the inverse gap function phase shift with respect to the selected reference.

In the case of dynamic eccentricity, the inverse gap function will have both even and odd harmonics which will cause (12) to have additional terms due to the interaction of the (p x odd) harmonics of both the inverse gap and the turns functions. As a result, the stator winding functions dc values, $< M_A >$, $< M_B >$ and $< M_C >$, will be a function of the rotor position angle, θ. However, the rotor winding function has a constant dc value, $< M_f >$, independent of the rotor position angle θ_m since the rotor coils rotate with the inverse gap function at the same rotational speed. When the air gap is symmetric, and no eccentricity exists, the inverse gap function has only (p x even) harmonics and the turns functions have only (p x odd) harmonics. Therefore, the winding functions will only have the ac components of the corresponding turns functions and the stator winding functions dc values will be simple constants.

In this study, up to the 10th harmonic were used for expressing the Fourier series of the inverse air gap function, the stator turns function and the rotor turns function. The inverse gap function has only the 4th and 8th harmonics since the 10th harmonic does not exist in the case of symmetric air gap. However, in the case of eccentric rotor all the odd and even harmonics could exist. In this case, 1st, 2nd, 3rd, 4th, 5th, 7th, 8th, 9th and 10th harmonics exist. The 6th harmonic and its multiples (or p x 3rd and its multiple) do not exist in this case, because the rotor pole arc is 60 mechanical degrees. In fact, for calculation of the machine mutual and magnetizing inductances, only even harmonics of the inverse gap function will participate because the integration of different frequency cosine multiplication over 2π cycle is zero. So, only 2nd, 4th, 6th, 8th and 10th harmonics of inverse gap function will have effect on the inductance calculations.

Figs. 6 and 7 show stator and rotor magnetizing inductance waveforms of the salient pole synchronous machine under study when the rotor is not and is experiencing dynamic eccentricity. It is clear that dynamic eccentricity will introduce new harmonic components in the inductances. The 2nd and the 10th harmonics will increase as level of dynamic eccentricity increases.

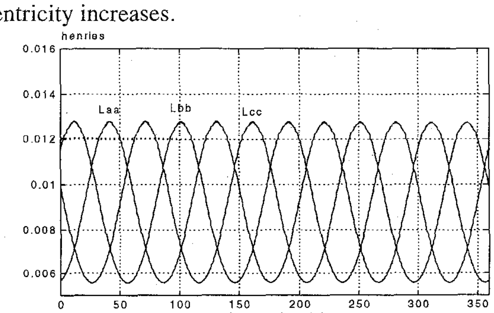

Fig. 6. Stator magnetizing inductances for symmetric air gap.

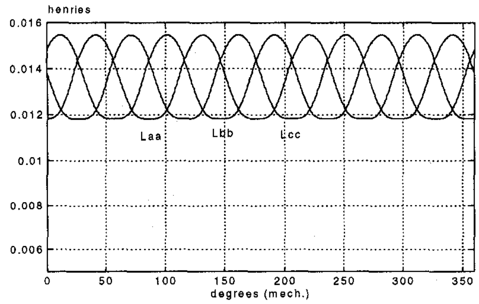

Fig. 7. Stator magnetizing inductances for the case of 85% dynamic eccentricity.

V. DYNAMIC MODEL OF THE SALIENT POLE SYNCHRONOUS MACHINES

The stator coupled magnetic circuit voltage equations can be written in vector-matrix form as follow

$$V_s = R_s I_s + \frac{d\Lambda_s}{dt} \tag{30}$$

where the stator flux linkages is given by

$$\Lambda_s = L_{SS} I_S + L_{SF} I_F \tag{31}$$

and

$$V_s = \begin{bmatrix} v_{as} & v_{bs} & v_{cs} \end{bmatrix}^t \quad , \quad \Lambda_s = \begin{bmatrix} \lambda_{as} & \lambda_{bs} & \lambda_{cs} \end{bmatrix}^t \quad , \quad I_s = \begin{bmatrix} i_{as} & i_{bs} & i_{cs} \end{bmatrix}^t$$

also

$$R_s = \begin{bmatrix} r_{as} & 0 & 0 \\ 0 & r_{bs} & 0 \\ 0 & 0 & r_{cs} \end{bmatrix}, L_{SS} = \begin{bmatrix} L_{saa} & L_{ab} & L_{ac} \\ L_{ba} & L_{sbb} & L_{bc} \\ L_{ca} & L_{cb} & L_{scc} \end{bmatrix}, L_{SF} = \begin{bmatrix} L_{af} \\ L_{bf} \\ L_{cf} \end{bmatrix}$$

where L_{saa}, L_{sbb}, and L_{scc} are the stator phases self inductances which are the summation of magnetizing inductances and leakage inductances. L_{ab} is the mutual inductance of stator phase a due to current in phase b. L_{af} is the mutual inductance of stator phase a due to the excitation current in rotor field winding, and etc..

Similarly, the rotor field voltage equation can be written in vector-matrix form as follow:

$$V_F = R_F I_F + \frac{d\Lambda_F}{dt} \tag{32}$$

and the rotor field flux linkages is represented by

$$\Lambda_F = L_{SF}{}^t I_S + L_{FF} I_F \tag{33}$$

where R_F is the rotor field resistance and L_{FF} is the rotor self inductance.

The magnetic co-energy equation can be used to find the electromagnetic torque equation as follow:

$$T_e = \left(\frac{\partial W_{CO}}{\partial \theta_{rm}} \right)_{(I_S, I_F \text{ constants})} \tag{34}$$

Since the co-energy is the energy stored in the magnetic circuits, it can be written as

$$W_{CO} = \frac{1}{2} I_S^t L_{SS} I_S + \frac{1}{2} I_S^t L_{SF} I_F + \frac{1}{2} I_F^t L_{SF}^t I_S + \frac{1}{2} I_F^t L_{FF} I_F \tag{35}$$

where θ_{rm} is the mechanical angle representing the rotor position.

VI. SIMULATION RESULTS

MATLAB mathematical package [9] was used for the dynamic simulation. All the machine inductances used for the simulation were expressed in their corresponding Fourier series. Two different simulation cases were created for conducting the analysis.

In the first case it was assumed that the rotor is not eccentric. The second case is similar to the previous case except that 50% dynamic rotor eccentricity was incorporated into the model to see the effect of eccentric rotor on the stator current signatures.

To analyze the stator currents signatures Fast Fourier Transform (FFT) of the current signals for both cases have been performed. Table 1 summarizes the percentage increase in the stator current harmonics due to dynamic eccentricity. It is clear that the 17th stator current harmonic has the highest relative percentage increase. The stator current signatures of synchronous machines can therefore be utilized for detecting dynamic eccentricity.

The stator current induced harmonics exist due to the interaction of magnetic fields produced by both the stator and rotor field windings. It is important to mention that in this study we have neglected slot openings, and therefore slot harmonics are not present. The air-gap magnetic field will generate harmonic fluxes that move relative to the stator, and therefore induce corresponding current harmonics in the stationary stator windings. These harmonic fluxes in the air-gap will increase as rotor dynamic eccentricity increases and consequently the current harmonic content increases further. The 3rd harmonic and its multiples do not exist in the stator windings because it is a three phase system with no neutral connection. However, the third harmonic components are induced in the rotor field windings.

Table 1: Relative percentage increase of stator harmonics due to 50% dynamic eccentricity.

5th	7th	11th	13th	17th	19th
22.8%	12.4%	20.9%	28.4%	47.1%	36.9%

VII. EXPRIMENTAL RESULTS

To study the effect of dynamic eccentricity on synchronous machines, an experiment has been performed on a round-rotor synchronous motor. The motor is a 3 phase, 1 kW, 208 V, 1.7 rated Amps and 1800 rpm synchronous motor. To conduct the experiment, the motor has been loaded separately with two different discs of the same size. The first disc has a smooth solid surface to emulate the case of non-eccentric rotor and the other disc has been drilled with four small holes on one side of it to realize an unbalanced disk. This unbalanced disk exacerbate the existing play in the bearings, and as a result rotor dynamic eccentricity will be induced.

The motor is first loaded with the smooth surface disc, and then the stator current and its frequency harmonics have been captured. To impose dynamic eccentricity on the rotor, the first disc coupled to the rotor shaft has been replaced with the second disc that has the drilled holes. Table 2 summarizes the relative percentage increase of stator current harmonics due to dynamic eccentricity. It is obvious again that the 17th stator current harmonic has the highest relative percentage increase

Table 2: Relative percentage increase of stator harmonics due to rotor eccentricity.

5th	7th	11th	13th	17th	19th
3.1%	3.2%	0.8%	70.0%	110.5%	52.74%

VIII. CONCLUSIONS

In this paper, the simple geometry and windings physical layout has been used for inductance calculations of a salient pole synchronous machine. Winding Function Approach presented earlier by previous researchers has been modified and expressed in general form to account for arbitrary winding distributions and air gap asymmetries during fault conditions. In fact, the Modified Winding Function Approach (MWFA) can be used for finding inductances of any electrical machine in cases of healthy and unhealthy conditions. The machine magnetizing and mutual inductances with and without rotor eccentricity were calculated using the MWFA. Also, dynamic simulation of the salient pole synchronous machine with and without rotor dynamic eccentricity were performed. Machine equations were obtained using the coupled magnetic circuit approach and simple geometry and windings physical layout.

The developed linear model was used to obtain machine stator current for both cases of symmetric and non-symmetric air gap. The computer simulations yield satisfactory results which are close to the machine ratings data provided by the manufacturer. Specific harmonic components have been increased in the stator currents that are associated with dynamic eccentricity. These harmonics can be detected to alarm for eccentric rotors. An experiment has been conducted on a around rotor synchronous motor and the results were found to be in a close agreement to the simulation results.

ACKNOWLEDGMENT

This material is based in part upon work supported by the Texas Advanced Research Program under Grant No. 95-P083 and by the Office of the Vice President for Research and Associate Provost for Graduate Studies, Texas A&M University. The authors would like to express their gratitude to Mr. William Dittman of Marathon Electric, Wausau, Wisconsin, for the assistance provided.

APPENDIX

Synchronous Motor Parameters:
4-pole, 475 kW, 480 V, 0.8 PF, 48 stator slots

L=273.05 mm	r=422.656mm
g=2.54 mm	Nr=108 turns/pole
Ns=3 turns/coil	Rs= .01592 Ω
Rr=.3632 Ω	8/12 pitch

REFERENCES

[1] P. J. Tavner, B. G. Gaydon and D. M. Ward, "Monitoring Generators and Large Motors," IEE Proc., vol. 133, pt. B, no. 3, pp. 169-180, May 1986.
[2] P J. Tavner, and J. Penman, *Condition Monitoring of Electrical Machines*. Letchworth, England: Research Press Limited, 1987.
[3] J. R. Cameron, W. T. Thomson, and A. B. Dow, "Vibration and Current Monitoring for Detecting Airgap Eccentricity in Large Induction Motors," *IEE Proc.*, vol. 133, pt. B, no. 3, pp. 155-163, May 1986.
[4] D. G. Dorrell, W. T. Thomson and S. Roach, "Analysis of Airgap Flux, Current and Vibration Signals as a Function of Combination of Static and Dynamic Airgap Eccentricity in 3-Phase Induction Motors," in *1995 IEEE Industry Applications Conference Records,* Orlando, Florida, vol. 1, pp. 563-570.
[5] P. Vas, *Parameter Estimation, Condition Monitoring, and Diagnosis of Electrical Machines*. Oxford: Clarendon Press, 1993.
[6] S. P. Verma, and R. Natarajan, "Effect of Eccentricity in Induction Motors," *Proc. of International Conference on Electrical Machines*, Budapest, Hungry, pp. 930-933, Sept. 1982.
[7] H. A. Toliyat, M. S. Arefeen and A. G. Parlos, "A Method for Dynamic Simulation and Detection of Air-Gap Eccentricity in Induction Machines," *IEEE Transactions on Industry Applications,* vol. 32, no. 4, pp. 910-918, Jul./Aug. 1996.
[8] J. S. Htsui, and J. Stein, "Shaft Signals of Salient-Pole Synchronous Machines for Eccentricity and Shorted-Field-Coil Detections," IEEE Trans. On Energy Conversion, vol. 9, no. 3, pp. 572-578, September 1994.
[9] MATLAB, mathematical packages by The MathWorks, Inc., Natick, MA.

Nabil A. Al-Nuaim (S'95) received the B.S. degree in electrical engineering in August 1991 from King Fahad University of Petroleum and Minerals at Dhahran, Saudi Arabia. In September 1991, he joined SCECO-East, the local power company, as a power system engineer where he was conducting power system analysis.

In September 1992, he joined the Consulting Services Department of Saudi Arabian Oil Company (Saudi Aramco) as an electrical engineer. He is currently pursuing the M.S.E.E at Texas A&M. Mr. Al-Nuaim was awarded the scholarship for graduate studies by Saudi Aramco.

Hamid A. Toliyat (S'87-M'91-SM'96) received the B.S. (1982) and M.S. (1986) in electrical engineering from Sharif University of Technology, Tehran, Iran and West Virginia University, Morgantown, WV, respectively. He received his Ph.D. degree in electrical engineering from the University of Wisconsin-Madison in 1991. In Fall of 1991 he joined the faculty of Ferdowsi University of Mashhad, Mashhad, Iran as an assistant professor of electrical engineering. Since 1994 he has been an assistant professor at the department of electrical engineering at Texas A&M University.

Dr. Toliyat is a Senior member of the Power Engineering, Industrial Applications, Industrial Electronics, and Power Electronics Societies of the IEEE, and the recipient of the 1996 IEEE Power Engineering Society Prize Paper Award for his paper on Analysis of Concentrated Winding Induction Machines for Adjustable Speed Drive Applications-Experimental Results. His main research interests and experience include fault diagnosis of electric machines, machine design and variable speed drives.